UC Davis
UC Davis Previously Published Works

Title

Methylation quantitative trait locus analysis of chronic postsurgical pain uncovers epigenetic mediators of genetic risk

Permalink

Journal

Epigenomics, 13(08)

ISSN

1750-1911

Authors

Chidambaran, Vidya
Zhang, Xue
Pilipenko, Valentina
et al.

Publication Date

2021-04-01

DOI

10.2217/epi-2020-0424

Peer reviewed

Methylation quantitative trait locus analysis of chronic postsurgical pain uncovers epigenetic mediators of genetic risk

Vidya Chidambaran*[,1] [ID], Xue Zhang[2], Valentina Pilipenko[2], Xiaoting Chen[3], Benjamin Wronowski[3], Kristie Geisler[1], Lisa J Martin[2,4], Artem Barski[2,3,4], Matthew T Weirauch[3,4] & Hong Ji[5]

[1]Department of Anesthesiology, Cincinnati Children's Hospital Medical Center, Cincinnati, OH 45229, USA
[2]Division of Human Genetics, Cincinnati Children's Hospital Medical Center, Cincinnati, OH 45229, USA
[3]Division of Allergy & Immunology, Cincinnati Children's Hospital Medical Center, Cincinnati, OH 45229, USA
[4]Department of Pediatrics, University of Cincinnati School of Medicine, Cincinnati, OH 45229, USA
[5]Department of Anatomy, Physiology & Cell biology, California National Primate Research Center, University of California, Davis, CA 95616, USA
*Author for correspondence: vidya.chidambaran@cchmc.org

Background: Overlap of pathways enriched by single nucleotide polymorphisms and DNA-methylation underlying chronic postsurgical pain (CPSP), prompted pilot study of CPSP-associated methylation quantitative trait loci (meQTL). **Materials & methods:** Children undergoing spine-fusion were recruited prospectively. Logistic-regression for genome- and epigenome-wide CPSP association and DNA-methylation-single nucleotide polymorphism association/mediation analyses to identify meQTLs were followed by functional genomics analyses. **Results:** CPSP (n = 20/58) and non-CPSP groups differed in pain-measures. Of 2753 meQTLs, DNA-methylation at 127 cytosine–guanine dinucleotides mediated association of 470 meQTLs with CPSP (p < 0.05). At PARK16 locus, CPSP risk meQTLs were associated with decreased DNA-methylation at *RAB7L1* and increased DNA-methylation at *PM20D1*. Corresponding *RAB7L1*/*PM20D1* blood eQTLs (GTEx) and cytosine–guanine dinucleotide-loci enrichment for histone marks, transcription factor binding sites and ATAC-seq peaks suggest altered transcription factor-binding. **Conclusion:** CPSP-associated meQTLs indicate epigenetic mechanisms mediate genetic risk.

Clinical trial registration: **NCT01839461, NCT01731873** (ClinicalTrials.gov).

Chronic postsurgical pain (CPSP) is a significant problem in children, with an incidence ranging from 14.5 to 38% [1–3]. Both genetic and environmental factors influence the risk for developing CPSP [4,5]. We recently conducted a systematic review of genetic variants associated with CPSP [6]. We found that well powered genome-wide association studies (GWAS) are scarce in CPSP, [7,8] and many of the SNPs described in genetic association studies [9–12] are located in noncoding regions, rendering functional interpretation difficult. The impact of environmental factors on the development of CPSP underscores the role of epigenetic mechanisms in the pathogenesis of acute to chronic pain transitions [13–15]. One widely studied epigenetic mechanism is DNA methylation. DNA methylation occurs primarily at CpG sites. DNA methylation influences gene expression without alterations to the underlying DNA sequence. Our previous epigenome-wide study in children undergoing spine fusion surgery showed that DNA methylation at CpG sites in genes enriching opioid, dopaminergic and GABA pathways was associated with CPSP [16,17]. Our systems biology guided study delineated genetic pathways involved in the pathophysiology of CPSP [18]. Interestingly, epigenetic pathways overlap with the genetic pathways enriched by gene variants associated with CPSP. Thus, we hypothesized that by integrating DNA methylation analyses with genetic studies, the mediating molecular mechanisms underlying CPSP can be elucidated [19].

Future Medicine

In the postgenome-wide association studies era, there is considerable interest in research focused on the influence of genetic polymorphisms (SNPs) on the level of DNA methylation at proximal CpG sites, also referred to as methylation quantitative trait loci (meQTLs) [20,21]. Identification of meQTLs provides putative mechanistic evidence for the role of noncoding genetic risk alleles with no known function. Additionally, they help identify molecular mechanisms – DNA methylation at specific CpG sites – that mediate the association between genotype and phenotype [22]. This is supported by the findings that meQTLs are located often at regulatory elements than expected by chance, providing credence to their ability to impact phenotype/disease risk by influencing transcription factor (TF) binding, chromatin conformation and gene expression [23,24]. This approach has been successfully utilized in a number of conditions, including schizophrenia, alcohol dependence, obesity, cancer, rheumatoid arthritis and metabolic traits [25–29].

In this pilot study, we aimed to identify meQTLs in blood that affect predisposition to CPSP through DNA methylation in a surgical cohort of adolescents with idiopathic scoliosis undergoing spine surgery. Understanding epigenetic-mediating mechanisms is crucial because while genetic variation (meQTL) cannot currently be modified, DNA methylation may be a modifiable risk factor.

Materials & methods

An observational prospective cohort study was conducted in adolescents with idiopathic scoliosis undergoing posterior spine fusion using standard surgical techniques, anesthetic and pain protocols. The studies are registered with ClinicalTrials.gov (identifier: NCT01839461, NCT01731873), and approved by the institutional review board. Written informed consent from parents and assent from children was obtained prior to enrollment. Pilot epigenome-wide and candidate DNA methylation study results from this cohort have been previously published [16,17].

Inclusion criteria

Children aged 10–18 years of American Society of Anesthesiologists physical status less than or equal to two (mild systemic disease) with a diagnosis of idiopathic scoliosis and/or kyphosis, scheduled to undergo elective spinal fusion.

Exclusion criteria

Females who were pregnant or breastfeeding; subjects with a diagnosis of chronic pain; opioid use in the past 6 months; hepatic/renal disease and/or developmental delays.

Data collection

Preoperatively, data were obtained on demographics (sex, age, race), weight, pain scores (Numerical Rating Scale/0-10; NRS) [30] and home medications. Questionnaires to assess anxiety sensitivity (childhood anxiety sensitivity index) [31] were administered preoperatively. All patients received total intravenous anesthesia (propofol and remifentanil) and midazolam in the intraoperative period followed postoperatively by standardized doses of patient-controlled analgesia (morphine or hydromorphone). Postoperatively, pain scores (every four hours) and doses of morphine equivalents administered on postoperative days one and two were recorded. At 6–12 months posthospital discharge, patients were asked to rate their average pain score (NRS) over the previous week. Data about psychologic questionnaires collected, anesthetic medications and pain (nature and location) for a larger cohort have been presented previously [32]. Here, we report on data relevant to this study's aims.

The primary outcome was incidence of CPSP, determined to be positive if a pain score >3/10 was reported on an 11-point NRS (range 0–10) 6–12 months after surgery. This cut-off was chosen because NRS pain scores >3 (moderate/severe pain) at three months have been described as a predictor for persistence of pain, associated with functional disability [33]. The NRS for pain intensity has been validated as a pain measure in children aged 7–17 years [30]. Occurrence of infection and malignancy in the interim period leading/contributing to chronic pain was ruled out.

Genotyping & measurement of DNA methylation

Blood samples were collected in EDTA tubes before surgery. DNA was isolated on the same day, and frozen at -80°C. Genotyping was done using the Illumina Human Omni5 v41-0 array (14 patients), Human Omni5Exome v41-1 (21 patients) and Infinium Omni5-4-v1 (39 patients). Arrays were changed due to availability of new array with more SNPs. SNPs from autosomal chromosomes were selected for analysis and annotated using ANNOVAR software [34].
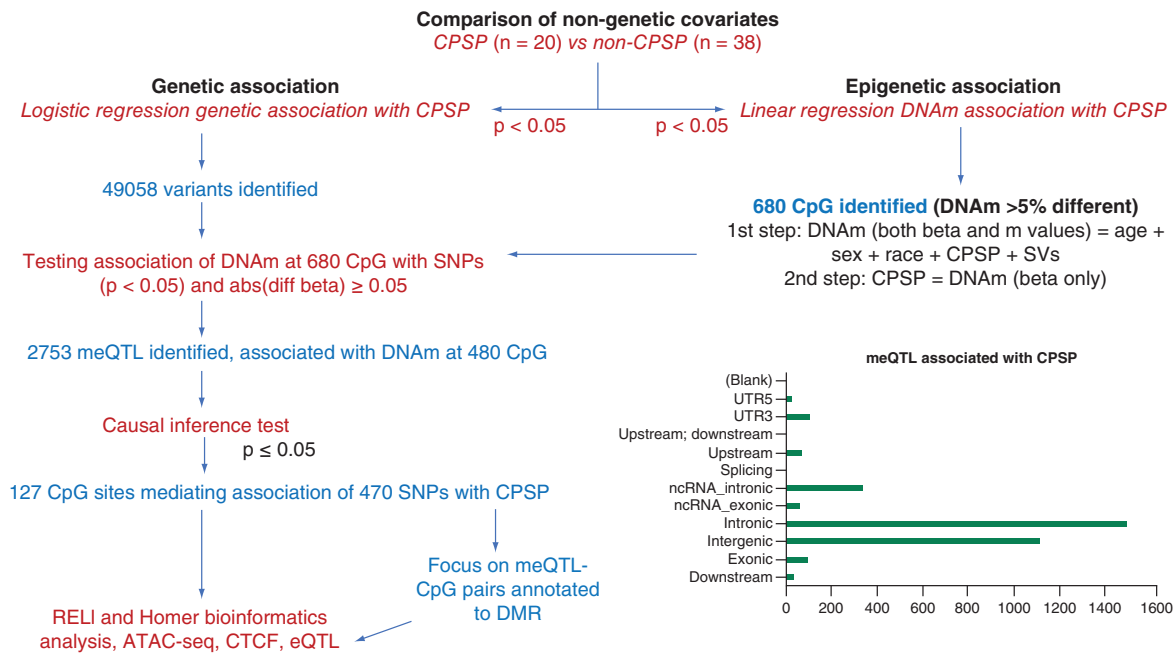
Figure 1.   Analysis workflow. Red text indicates tests; blue text indicates results.

All samples passed 95% threshold for call rates at genotype and individual levels. Genetic data was assessed for Hardy–Weinberg equilibrium by means of a goodness of fit χ^2 test with threshold for p-values 0.0001. Low-frequency variants were also excluded – the threshold for minor allele frequencies was 10% (Supplementary Figure 1 for quality control workflow). DNA methylation was measured using using Zymo EZ DNA Methylation Gold kit (Zymo Research, CA, USA), as described previously [16]. Data were then quality-controlled and preprocessed as previously described. Both beta and M-values were obtained and used. To control for unwanted variation and potential batch effects, surrogate variables were obtained using the R package 'sva' and included as co-variables in relevant analyses. Illumina annotation was used for data interpretation, for example, probe location within genes, CpG islands and shores, and regulatory features (http://genome.ucsc.edu; UCSC Genome Bioinformatics, CA, USA).

Data analysis

The clinical characteristics, demographics and pain variables of the cohort were described using mean (with standard deviation), median interquartile range and frequency (percentage) depending on data distribution. The CPSP and non-CPSP groups were compared for non-genetic factors including demographics, surgical duration and childhood anxiety sensitivity index using statistical methods appropriate for the distribution of the data. Factors significantly different between groups ($p < 0.05$) were included as covariates for further genetic/epigenetic association analyses. Since preoperative pain and acute postoperative pain are correlated with CPSP as primary pain outcomes, with possible overlap of DNA methylation associations, we did not consider them as co-variables in the multivariate genetic/DNA methylation models for CPSP. An overview of the analytic workflow is provided in Figure 1.

Genetic & DNA methylation association analyses

Analyses were conducted using PLINK version 1.9 [35]). To identify genetic variants that were significantly associated with presence/absence of CPSP for each of the variants, logistic regression was performed, assuming additive genetic effects in which genotypes were numerically coded according to the number of minor alleles. Variants associated with CPSP at $p < 0.05$ were selected for further analyses. DNA methylation association with *CPSP*: The beta and M-values were first regressed against CPSP with age, sex, race and corresponding SVs controlled using the R package 'limma'. CpG sites whose methylation significantly ($p < 0.05$) differed by 5% between CPSP and non-CPSP were the steps selected. Associations between these CpG sites and CPSP were then confirmed by logistic regression using
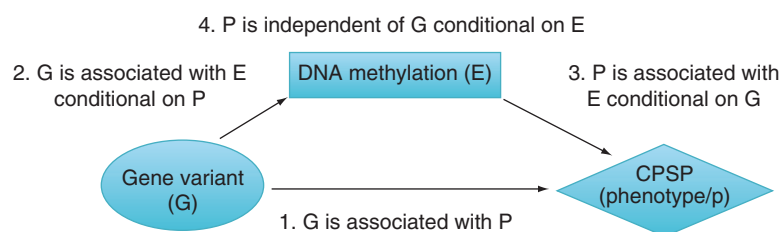
Figure 2.   Causal inference test steps. Omnibus test: intersection/union test for p-value of causal interference test.

CPSP as the dependent variable. Only CpGs that showed significantly association in the logistic regression were used in subsequent analyses.

meQTL analysis

Using the R package 'MatrixEQTL' [36], meQTLs were identified by regressing DNA methylation of the significant CpG sites against the genotypes of the genetic variants. For methylation levels of each SNP-CpG pair, linear regression was performed assuming additive genetic effects. Age, sex, race (White vs non-White) and SVs were adjusted as co-variables. meQTL were selected if DNA methylation (measured by both beta and M-values) and genotype associated at $p < 0.05$ level, and one copy of the minor allele led to a 5% change or more in DNA methylation.

Causal inference test for mediation analysis

The causal inference test (CIT) is based on hypothesis testing rather than estimation, allowing the testable assumptions to be evaluated in the determination of statistical significance [37]. All meQTLs selected in the steps above were included in the CIT performed using the R package 'CIT' to select meQTLs whose association with CPSP was significantly mediated by DNA methylation ($p < 0.05$). The steps are illustrated in Figure 2 (https://cran.r-project.org/web/packages/cit/index.html) [38].

Functional genomics analysis

To identify epigenetic marks and TF binding events that are enriched at 5mC sites, we used a computational method we have described previously [39] where the set of genomic locations with 5mC marks were overlapped with a large collection of functional genomics datasets from ENCODE [40], Roadmap Epigenomics [41] and chromatin immunoprecipitation (ChIP)-seq for histone marks [42].

All datasets were indexed by their genomic coordinates, which were used to intersect with the genomic coordinates of methylation sites of interest. Using RELI [43], the significance of such intersections was estimated by comparing to a null model, which consists of regions with 5mC (beta >0.2) but no significant association with CPSP (control) and those associated with CPSP ($p > 0.05$ AND absolute paired difference <0.2). The expected intersection values from the null model was normally distributed. The model parameters were estimated and the significance of the observed number of intersections, for example, a Z-score and the corresponding p-value was calculated for the observed intersections of methylation sites of interest. This procedure controls for the count and sizes of the input loci and each individual dataset in the library. Genomic loci with 5mC marks were also examined using standard TF motif enrichment analysis. using HOMER motif enrichment algorithm [44] and human position weight matrix binding site models from the CisBP database [45] as described before [39].

Focus on meQTL-CpG pairs (significant by CIT) annotated to differentially methylated regions (DMR) by Illumina: due to our focus on meQTL in this manuscript, we did not conduct DMR analysis. Instead we focused on DMR annotations by Illumina which were enriched for meQTL-CpG pairs. We evaluated HOMER/RELI findings overlapping CpG sites at these locations. We also used the Genotype-Tissue Expression portal to identify correlations between genotypes of meQTLs and blood gene expression levels to determine if direction of effects on DNA methylation were consistent with reported computed expression quantitative trait loci (eQTLs). We conducted Assay for Transposase-Accessible Chromatin using sequencing (ATAC-seq) on isolated monocytes from

Table 1. Demographic, perioperative and pain data for the entire cohort, subjects who developed chronic postsurgical pain (chronic postsurgical pain yes) and those who did not (chronic postsurgical pain no).

Variable	All (n = 74)	CPSP no (n = 38)	CPSP yes (n = 20)	p-value
Age (year)	14.4 ± 1.7	14.4 ± 1.8	14.9 ± 1.4	0.24[†]
Sex (male)	11 (14.9%)	7 (18.4%)	1 (5%)	0.24[‡]
Race (White)	59 (79.7%)	31 (81.6%)	16 (80.0%)	1.00[‡]
Weight (kg)	53.7 (50.4–57.2)	53.7 (50.8–58.5)	53.8 (50.0–58.0)	0.88[§]
CASI	28.9 ± 5.5	27.5 ± 5.1	30.0 ± 5.5	0.15[†]
Preoperative pain score	0.0 (0.0–0.0)	0.0 (0.0–0.0)	0.0 (0.0–2.0)	0.010[§]
Surgical duration	4.3 ± 1.1	4.3 ± 1.0	3.9 ± 1.2	0.20[†]
Pain AUC POD 1 and 2	207.0 ± 82.8	185.6 ± 75.2	242.0 ± 88.9	0.024[†]
Morphine dose POD 1 and 2 (mg/kg)	1.3 (0.9–1.9)	1.3 (1.0–1.8)	1.5 (1.1–2.3)	0.22[§]
Pain scores at 6–12 months	1.0 (0.0–4.0)	0.0 (0.0–6.0)	5.0 (4.0–6.0)	<0.001[§]

[†] t-test;
[‡] Fisher's exact test;
[§] Wilcoxon rank sum test.
AUC: Area under curve; CASI: Childhood Anxiety Sensitivity Index; CPSP: Chronic postsurgical pain; POD: Postoperative day.

one patient (Phenotype: CPSP) to show evidence for open accessibility in meQTL-CpG enriched DMR (by annotation) associated with CPSP. Using fresh blood (7 ml) collected preoperatively, white blood cells were purified by HESPAN sedimentation, aliquoted and viably frozen in serum/DMSO solution. This protocol produces >80% viable cells upon thawing. Since DNA accessibility is affected by cell composition, we performed ATAC-seq on $CD14^+$ monocytes negatively selected using magnetic kits from Stem Cell. This cell subset preference is based on evidence of differential immune signatures correlated to pain in patients undergoing hip arthroplasty [46,47]. We performed Tn5 reaction using OMNI-ATAC [48] protocol on 50 K magnetically purified cells. Libraries were amplified and submitted for Illumina sequencing at Novagene (PE150, ~20 M reads). Data analysis was performed using SciDAP platform (https://scidap.com, Datirium, LLC) [49]. Containerized CWL pipelines are available at https://github.com/datirium/workflows. Briefly, trimmed ATAC reads were aligned to the human genome using Bowtie [50] extended to 9 bp, normalized to total mapped read number and displayed as coverage on IGV-JS genome browser built into SciDAP. MACS2 was used to identify islands of enrichment [51].

Results

We recruited 74 participants for the study. The mean age of participants was 14.4 years (standard deviation 1.7); they were mostly White (79.7%) and female (85.1%). A description of pain and other variables is provided in Table 1. Follow-up for CPSP outcomes was successful for 58 of these subjects (loss to follow-up 16/74–21.6%). Incidence of CPSP in this cohort was 20/58 (34.5%). Preoperative pain, acute postoperative pain and pain at 6–12 months were significantly higher in the CPSP group compared with the non-CPSP group. None of the other factors were identified to be significantly different by univariate analysis (p < 0.05).

Genetic & DNA methylation association with CPSP

The following quality control – exclusion workflow (Supplementary Figure 1) was utilized: 121,301 SNPs from the sex chromosome, chromosome zero, mitochondrial, indels and other were excluded from analysis. SNPs that failed Hardy–Weinberg Equilibrium (p < 0.0001) or had minor allele frequencies below 10% were excluded. There were 4,186,587 variants on the exome chip initially and 1,270,531 variants remained after exclusion by QC. A total of 49,058 SNPs were nominally associated with CPSP (p ≤ 0.05). The results are enumerated according to the analytic workflow in Figure 1. Following QC, 842,148 CpG sites were deemed evaluable. DNA methylation (both beta and M-values) at 680 CpG sites were found to be associated with CPSP (p < 0.05 and >5% difference in beta values).

meQTL (SNP-CpG-DNA methylation association) underlying CPSP

Pairwise association of the 49,058 variants with DNA methylation at 680 CpG sites identified 2753 meQTL with significant impact on the DNA methylation levels (≥5% change) at 480 CpG sites. Less than 100 of the meQTLs identified were exonic (inset, Figure 1), with the majority being located in intronic or intergenic regions.

CIT results

After CIT, 529 variant-CpG associations were found, with 127 unique CpG sites potentially mediating the genetic association of 470 variants with CPSP. The relation of the CpG sites location in relation to CpG islands per the UCSC browser was available for 57.5% of the 127 sites (26.0% were located in a CpG island, 12.6% in the north shore of the islands, 15.7% in the south shore and 1.6% each in north and south shelves. Details of CpG-meQTL pairs significant by CIT are presented in Supplementary Table 1. Descriptions of meQTL with SNP annotations from ANNOVAR, CpG site details, CIT results, association of DNA methylation at the site and Odds ratio for meQTL with CPSP are tabulated.

Functional genomics

To better understand the potential functions of the 127 CpGs identified by the CIT, functional genomics analyses was used to identify enriched epigenetic markers (e.g., histone marks) and TF-binding motifs (see Methods). These analyses revealed strong enrichment for repressive (H3K27me3 and H3K9me3) and active (H3K4me1) histone marks, in addition to eQTLs, consistent with these regions being located within regulatory regions in brain-derived, and other tissues (Figure 3A). Further analysis revealed enrichment for binding sites for particular TFs, including MAF, KLF1, FOXC1 and GATA1, at these loci (Figure 3B).

PARK16 locus CpG-DNA methylation associations

We focused on meQTL-CpG DNA methylation pairs significant by CIT, annotated to DMR by Illumina. Interestingly, 18 of such 26 meQTL-CpG DNA methylation associations were between meQTLs at PARK16 locus and CpG sites on PARK16 locus (DNA methylation at *RAB7L1* CpG sites annotated to a DMR, and CpG sites on *PM20D1*) (Figure 4). PARK16 locus is a genetic region spanning five genes on chromosome 1q32. The five genes that make up the PARK16 locus include *SLC45A3*, *NUCKS1*, *RAB7,RAB7L1*, *SLC41A1*, and *PM20D1*.

meQTLs on genes *NUCKS1* (rs4951261, rs823114, rs823130, rs11240565), PM20D1 (rs960603), RAB29 (rs708723), SLC45A3 (rs16856110, rs2793374, rs11240547), SLC41A1 (rs1772159), *SLC45A3/NUCKS1* (rs1172198, rs823096, rs823105) and *ELK4/SLC45A3* (rs11589772) were associated with DNA methylation on CpG sites in the north shore of CpG islands on *RAB7L1* and sites on south shore of CpG islands on *PM20D1*. The level of DNA methylation in shores has previously been shown to be more highly correlated with gene expression than that of CpG islands likely because of transcription machinery binding to nearby promoter CpG islands [52]. DNA methylation at CpG sites on *RAB7L1* were uniformly hypomethylated and *PM20D1* CpG sites were uniformly hypermethylated in association with high risk CPSP genotypes. Beta values for association of CpG-DNA methylation with CPSP and meQTL associated odds for CPSP risk in the PARK16 region are provided in Table 2. Representative meQTL (rs708723 (*RAB29*) and rs960603 (*PM20D1*) genotypes)-CpG (cg 16031515 on *RAB7L1* and cg16334093 on *PM20D1*) DNA methylation with superimposed CPSP phenotypes are shown in Figure 5. Description of meQTL, the CpG sites whose DNA methylation they affect, p-values of CIT components, and association of meQTL with DNA methylation at the CG sites for the PARK16 locus are tabulated in Table 3. Examples of meQTL associations with CPSP mediated by CpG sites in PARK16 are illustrated in Figure 6. Directions of association of meQTL-DNA methylation at CpG sites and CPSP is consistent with risk genotypes. Higher *PM20D1* DNA methylation mediates meQTL association with higher CPSP risk. Risk genotypes are associated with decreased DNA methylation at *RAB7L1* CpG sites; however, since DNA methylation at *RAB7L1* sites are independently protective of CPSP, hypomethylation at *RAB7L1* mediates association of meQTL with higher risk for CPSP.

Functional genomics: PARK16

RELI analyses showed significant overlap (p < 0.001) overlap for transcription factor binding sites (TFBS) (for GATA2, IKZF1 and INO80) at CpG sites with differential DNA methylation at PARK16 loci (*RAB7L1* and *PM20D1*). These results indicate that these particular TFs might have altered binding events due to differential methylation. eQTLs for rs708723 (*RAB7L1*), rs960603 (*PM20D1*) and rs823114 (*NUCKS1*) genotypes accessed through G-TEx portal are shown in Supplementary Figure 2. Consistent with expected expression based on DNA methylation associations with meQTLs, we found significantly higher *RAB7L1* and lower *PM20D1* eQTLs associated with high risk genotypes, but no eQTLs for other genes in PARK16 (*SLC41A1* and *NUCKS1*).
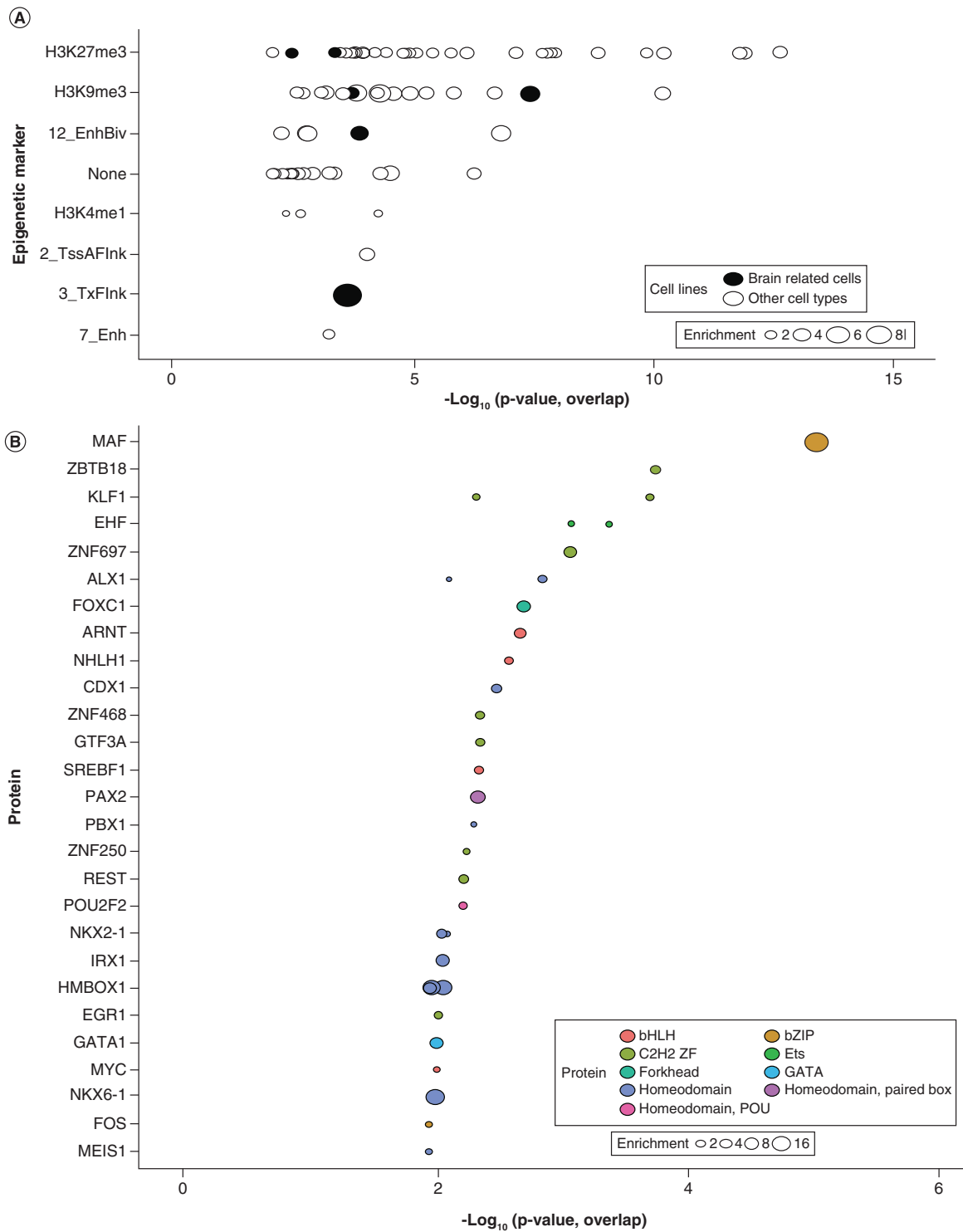
Figure 3. Enriched gene regulatory mechanisms within the 127 CpGs that causally mediate associations between SNPs and chronic post surgical pain. (A) Epigenetic markers enriched within these regions – histone marks, expression trait quantitative loci, and chromatin states. The X-axis indicates the significance (-log p-value), using the RELI software package (see Methods). The size of each circle indicates the fold-enrichment relative to background. Chromatin states are based on combinations of histone marks using the ChromHMM tool and data from RoadMap Epigenomics: 12_EnhBiv, bivalent enhancer; 2_TssAFlnk, region flanking an active transcription start site; 3_TxFlnk, transcribed regions; 7_Enh, enhancer. **(B)** Transcription factor binding site motifs enriched within the DNA sequences of these regions. The Y-axis indicates regulatory proteins (e.g., transcription factors), in decreasing order of significance.
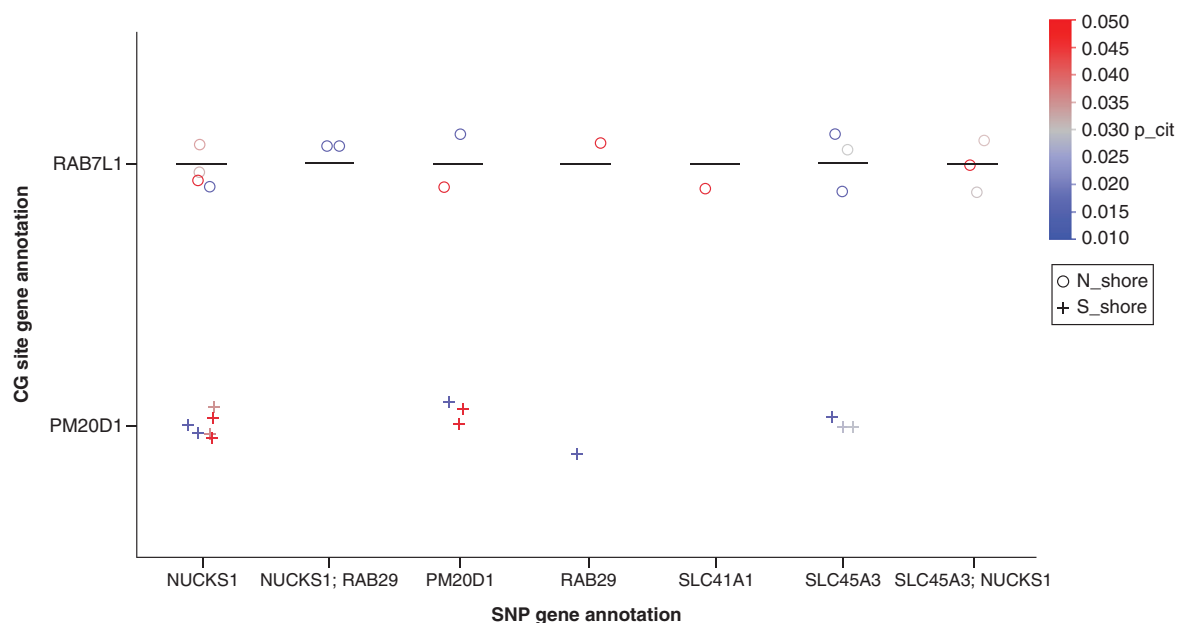
Figure 4.   Differentially methylated CpG sites - meQTL pairs associated with chronic post-surgical pain in the PARK16 locus.

Table 2. CG sites, methylation quantitative trait loci and chronic postsurgical pain associations at the PARK16 locus.								
CpG	CHR	Location genome build 37/Hg19	Relation to CpG island	Gene	p-value: DNAm step 1[†] beta	Difference in beta: CPSP yes vs no	DNAm Step 2[‡] p-value DNAm-CPSP	Snp-CpG
cg16031515	1	205743344	N_Shore	RAB7L1	0.004	-0.106	0.005	N
cg26418147	1	205743515	N_Shore	RAB7L1	0.003	-0.073	0.002	N
cg14893161	1	205819251	S_Shore	PM20D1	0.018	0.129	0.007	N
cg12898220	1	205819356	S_Shore	PM20D1	0.039	0.13	0.007	N
cg11965913	1	205819406	S_Shore	PM20D1	0.009	0.157	0.007	N
cg07167872	1	205819463	S_Shore	PM20D1	0.02	0.152	0.003	N
cg16334093	1	205819600	S_Shore	PM20D1	0.029	0.099	0.005	N
cg07157834	1	205819609	S_Shore	PM20D1	0.017	0.099	0.005	N
meQTL	Risk allele	CHR	Location	Function	Gene	Odds ratio	LL 95% CI	UL 95% CI	p-value
rs16856110	G	1	205631767	intronic	SLC45A3	0.218	0.055	0.870	0.031
rs11240547	A	1	205632932	intronic	SLC45A3	0.387	0.159	0.945	0.037
rs2793374	A	1	205647508	intronic	SLC45A3	3.626	1.456	9.030	0.006
rs823105	A	1	205657570	intergenic	SLC45A3; NUCKS1	4.032	1.611	10.090	0.003
rs1172198	A	1	205662718	intergenic	SLC45A3; NUCKS1	4.679	1.755	12.470	0.002
rs823096	A	1	205679887	intergenic	SLC45A3; NUCKS1	4.051	1.592	10.310	0.003
rs823130	A	1	205714372	intronic	NUCKS1	5.944	1.933	18.270	0.002
rs4951261	C	1	205717823	intronic	NUCKS1	0.338	0.136	0.842	0.020
rs823114	A	1	205719532	upstream	NUCKS1	2.881	1.252	6.630	0.013
rs11240565	A	1	205722958	intergenic	NUCKS1; RAB29	0.376	0.157	0.902	0.028
rs708723	A	1	205739266	UTR3	RAB29	3.194	1.345	7.586	0.009
rs1772159	A	1	205759195	UTR3	SLC41A1	6.020	1.907	19.000	0.002
rs960603	A	1	205812614	intronic	PM20D1	4.866	1.382	17.130	0.014

[†]Step 1 (DNA methylation association): DNAm (DNA methylation) beta values = age + sex + race + CPSP + surrogate variables.
[‡]Step 2 (DNAm-CPSP association): CPSP = DNAm (beta values).
meQTLs that have increase risk for CPSP (odds ratio >1) are not shaded in the lower table.
CHR: Chromosome; CpG: Cytosine–guanine dinucleotide; CPSP: Chronic postsurgical pain; DNAm: DNA methylation; meQTL: Methylation quantitative trait loci.

Table 3. Causal inference test results for association of methylation quantitative trait loci with CPSP mediated by DNAm at the CG sites in PARK16 locus.

| SNP | Chr 1 location | meQTL | | CpG | | p-values | | | | | | meQTL-CG ass | |
		Function	Gene	CG	Gene	CIT	PassG	PassG/E	EassG/P	GIndP/E	Beta	T-stat	p-value
rs16856110	205631767	intronic	SLC45A3	cg16031515	RAB7L1	0.025	0.018	0.021	0.000	0.025	0.156	5.335	0.000
rs11240547	205632932	intronic	SLC45A3	cg07167872	PM20D1	0.028	0.028	0.010	0.000	0.011	-0.213	-5.080	0.000
rs11240547	205632932	intronic	SLC45A3	cg12898220	PM20D1	0.029	0.028	0.029	0.000	0.025	-0.201	-4.847	0.000
rs2793374	205647508	intronic	SLC45A3	cg26418147	RAB7L1	0.022	0.003	0.017	0.000	0.022	-0.082	-6.838	0.000
rs2793374	205647508	intronic	SLC45A3	cg11965913	PM20D1	0.026	0.003	0.026	0.000	0.016	0.201	5.872	0.000
rs823105	205657570	intergenic	SLC45A3;NUCKS1	cg26418147	RAB7L1	0.033	0.001	0.033	0.000	0.032	-0.090	-7.936	0.000
rs1172198	205662718	intergenic	SLC45A3;NUCKS1	cg26418147	RAB7L1	0.050	0.000	0.050	0.000	0.043	-0.088	-7.622	0.000
rs823096	205679887	intergenic	SLC45A3;NUCKS1	cg26418147	RAB7L1	0.031	0.001	0.031	0.000	0.030	-0.091	-8.302	0.000
rs823130	205714372	intronic	NUCKS1	cg26418147	RAB7L1	0.037	0.000	0.028	0.000	0.037	-0.092	-7.916	0.000
rs4951261	205717823	intronic	NUCKS1	cg26418147	RAB7L1	0.012	0.012	0.006	0.000	0.005	0.075	6.570	0.000
rs4951261	205717823	intronic	NUCKS1	cg16031515	RAB7L1	0.034	0.012	0.034	0.000	0.025	0.117	6.937	0.000
rs4951261	205717823	intronic	NUCKS1	cg07167872	PM20D1	0.016	0.012	0.016	0.000	0.009	-0.191	-5.564	0.000
rs823114	205719532	upstream	NUCKS1	cg16031515	RAB7L1	0.039	0.008	0.027	0.004	0.039	-0.102	-5.526	0.000
rs823114	205719532	upstream	NUCKS1	cg07157834	RAB7L1	0.041	0.008	0.041	0.000	0.027	0.142	6.989	0.000
rs823114	205719532	upstream	NUCKS1	cg16334093	PM20D1	0.047	0.008	0.047	0.000	0.028	0.151	6.809	0.000
rs823114	205719532	upstream	NUCKS1	cg14893161	PM20D1	0.037	0.008	0.037	0.000	0.025	0.186	6.635	0.000
rs823114	205719532	upstream	NUCKS1	cg11965913	PM20D1	0.015	0.008	0.015	0.000	0.002	0.200	6.422	0.000
rs823114	205719532	upstream	NUCKS1	cg07167872	PM20D1	0.036	0.008	0.036	0.000	0.032	0.233	7.756	0.000
rs11240565	205722958	intergenic	NUCKS1;RAB29	cg26418147	RAB7L1	0.019	0.019	0.004	0.000	0.009	0.076	6.433	0.000
rs11240565	205722958	intergenic	NUCKS1;RAB29	cg16031515	RAB7L1	0.024	0.019	0.024	0.000	0.019	0.124	7.345	0.000
rs708723	205739266	UTR3	RAB29	cg16031515	RAB7L1	0.047	0.004	0.033	0.005	0.047	-0.105	-5.584	0.000
rs708723	205739266	UTR3	RAB29	cg11965913	PM20D1	0.023	0.004	0.023	0.000	0.011	0.206	6.520	0.000
rs1772159	205759195	UTR3	SLC41A1	cg26418147	RAB7L1	0.044	0.000	0.040	0.000	0.044	-0.099	-8.079	0.000
rs960603	205812614	intronic	PM20D1	cg16031515	RAB7L1	0.040	0.005	0.027	0.008	0.040	-0.145	-5.923	0.000
rs960603	205812614	intronic	PM20D1	cg26418147	RAB7L1	0.013	0.005	0.004	0.013	0.012	-0.092	-5.559	0.000
rs960603	205812614	intronic	PM20D1	cg14893161	PM20D1	0.047	0.005	0.047	0.000	0.026	0.263	7.116	0.000
rs960603	205812614	intronic	PM20D1	cg11965913	PM20D1	0.021	0.005	0.021	0.000	0.018	0.296	7.453	0.000
rs960603	205812614	intronic	PM20D1	cg07167872	PM20D1	0.045	0.005	0.045	0.000	0.035	0.302	7.066	0.000

The p-values for the causal inference test are based on the following:
Genetic locus (G), epigenetic/DNAm locus (E) as a potential mediator of an effect of L on CPSP phenotype (P), then the conditions are: G is associated with P, G is associated with E conditional on P, P is associated with E conditional on G and P is independent of G conditional on E. A p-value is computed for each condition using a general linear modeling framework, and the maximum p-value is interpreted as an omnibus hypothesis test (the causal inference test/CIT) for the intersection of the component rejection regions, an 'intersection/union test'. The association between a CG and an SNP (to identify meQTL) shows the regression coefficient (beta), t-statistic and p-value. The shaded rows correspond with the meQTLs which were associated with decreased risk of CPSP. Notably, the direction of their effect on DNAm at same CpG sites is opposite to the meQTLs which increase CPSP risk.
CpG: Cytosine–guanine dinucleotide; CPSP: Chronic postsurgical pain; DNAm: DNA methylation; meQTL: Methylation quantitative trait loci; SNP: Single nucleotide polymorphism.
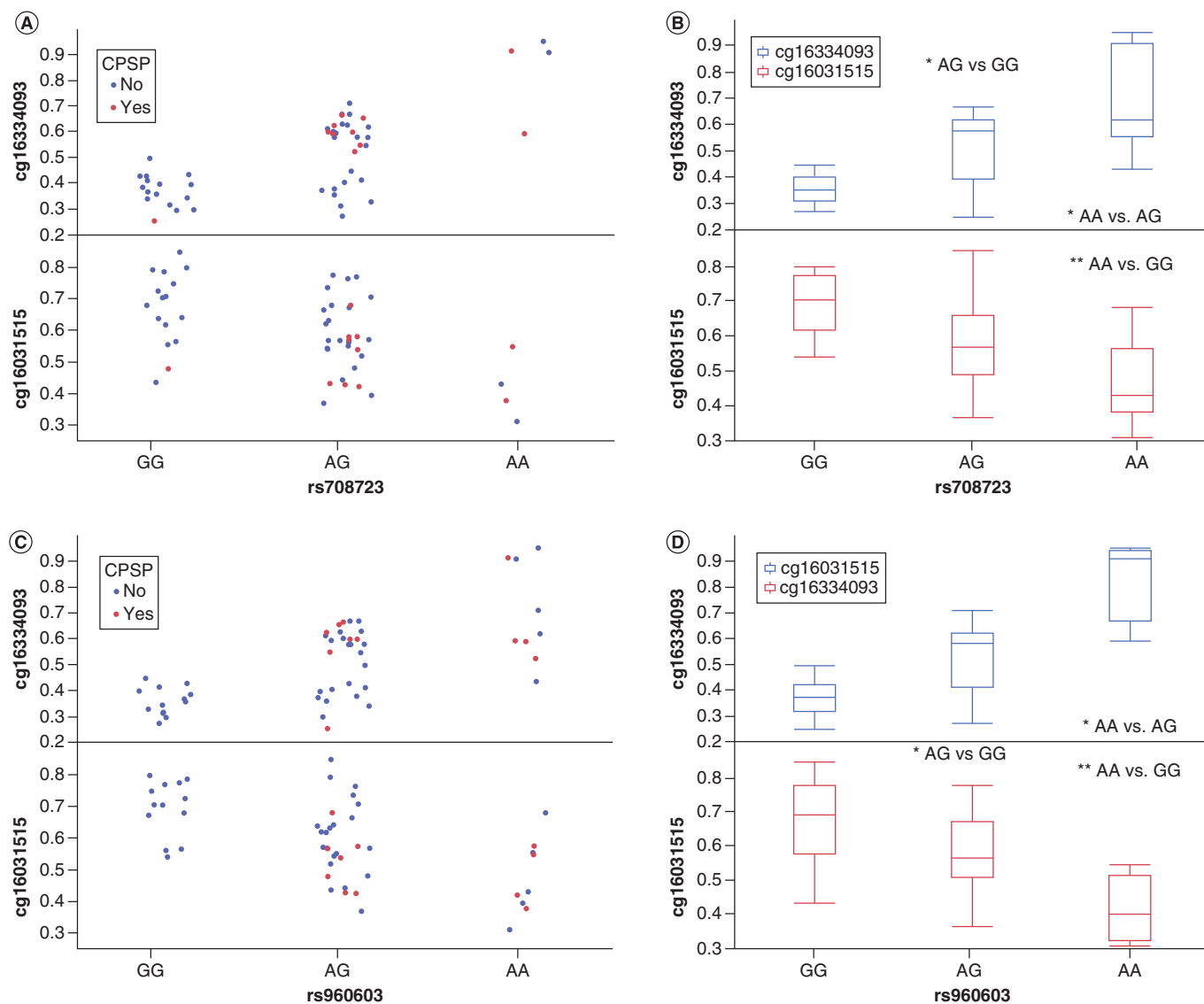
DNAm: DNA methylation; CPSP: Chronic post surgical pain.

ATAC-seq: PARK16

We identified chromatin accessibility peaks in PARK16 locus genes overlapping mediating CpG sites as well as meQTLs associated with CPSP (Supplementary Figure 3). For example, Chr1: 205819055–205819458 in *PM20D1* shows a broad ATAC-seq peak overlapping 6 CpG sites (Chr1:205819251–205819609) indicating open chromatin regions amenable to be affected by DNA methylation changes leading to altered TF binding. Also shown are overlapping CTCF peaks in monocytes (CD14$^+$ cells) from publicly available ENCODE dataset (EH002169, GSM1022659). This includes a previously reported CTCF peak at Chr1: 205,760,411–205,761,320 in the *SLC41A1* gene transcription end site, about 17 kb from the CpG sites annotated to CpG sites on *RAB7L1* (Chr1: 205743344–205743515) and about 60 kb away from the differentially methylated CpG sites enriching south shore of CpG islands on *PM20D1* (Chr1: 205819251–205819609).

Discussion

In this pilot study, by integrating genotype and DNA methylation analyses, we identified 2753 putative meQTLs associated with CPSP. In addition, DNA methylation at 127 CpG sites were found to mediate associations between 470 SNPs and CPSP. The PARK16 locus on Chromosome 1 was identified as a primary site with several meQTL-CpG associations. The association of meQTLs annotated to genes in the PARK16 genetic locus with CPSP were
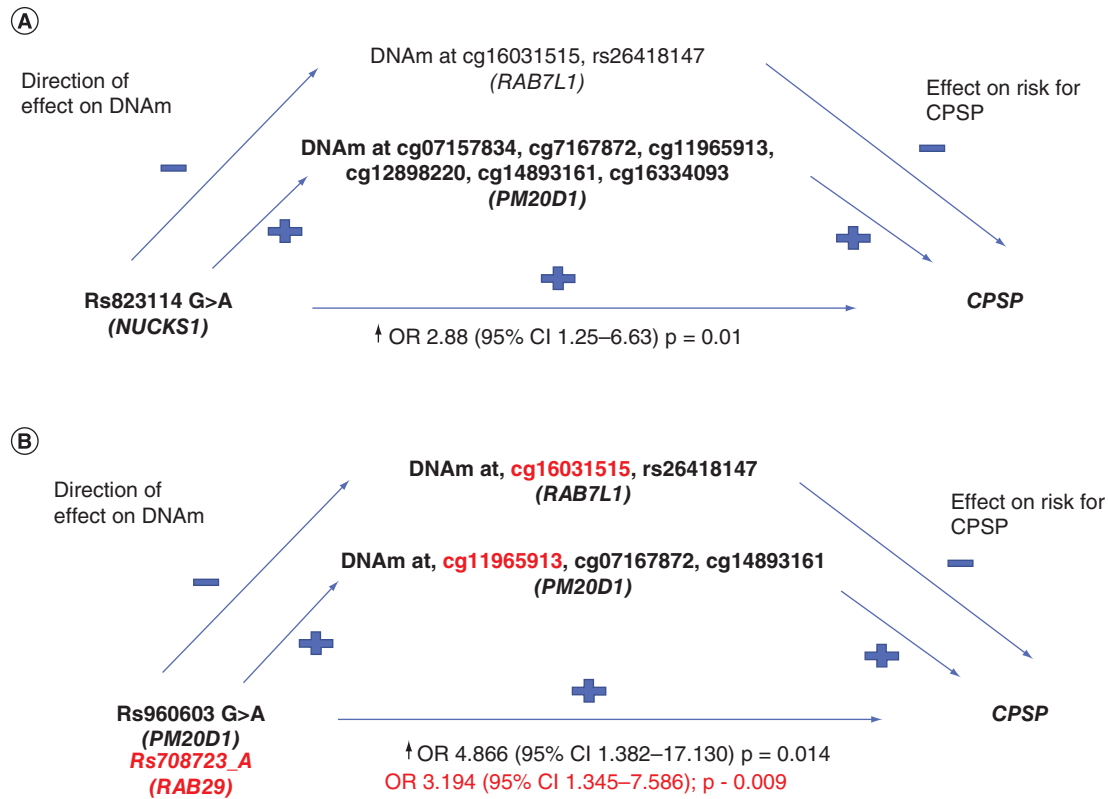
Figure 6.   Mediation model showing mediation of meQTL association with chronic post surgical pain by DNA methylation. Mediation model denoting mediation by DNAm at CpG sites on two genes (RAB7L1 and PM20D1) of association of meQTLs rs823114 G_A (NUCKS1) **(A)**, rs960603 G_A (PM20D1) and rs708723 (RAB7L1) **(B)** with CPSP. Odds ratios for CPSP (all meQTLs are associated with increased Odds for CPSP) are presented. Causal inference test was significant for all these interactions. The direction of association of meQTL on DNAm and DNAm on CPSP are denoted by + (positive) and - (negative) signs. In panel B, the red font indicates specific additional CpG sites affected by meQTL rs708723. Net effect of all meQTLs was to decrease DNAm at RAB7L1 sites and thus decreased the protective effect of RAB7L1 CpG DNAm on CPSP, and to increase DNAm at PM20D1 associated with increased risk for CPSP. CPSP: Chronic post-surgery pain; DNAm: DNA methylation; OR: Odds ratio.

found to be mediated by reprogramming-specific differentially methylated regions on two genes in the same region (*RAB7L1* and *PM20D1*). meQTLs associated with risk of CPSP were consistently associated with decreased DNA methylation at *RAB7L1* and increased DNA methylation at *PM20D1* CpG sites. In the absence of cell- and tissue-specific experimental evidence, our functional data interpretation provides putative evidence that differential methylation at the CpG sites modulates binding of TFs and might represent the possible mechanism underlying the regulatory effects of some noncoding gene variants on CPSP development.

The genomic methylation pattern at PARK16 locus has been found to be associated with neurodegenerative conditions such as Parkinson's disease and Alzheimer's disease [53–57]. This is the first time this region is shown to be associated with molecular mechanisms linked to acute to chronic pain transition. Although there is no direct evidence for the role of PARK16 in chronic pain, we know that parkinson's disease (PD) is associated with chronic pain and abnormal pain processing [58]. We also know that dopamine deficit lowers multimodal pain thresholds and dopaminergic mechanisms underly pain, depression, and addiction [59]. Our previous findings – differential DNA methylation in regulatory genomic regions enriching GABA and dopamine DARPP32 signaling pathways associated with CPSP and anxiety sensitivity in adolescents undergoing spine surgery – also suggested dopamine-related emotion/reward contributes to behavioral maintenance of pain after surgery [16]. Notably, methylation changes have been described to be consistent in brain and blood for this genomic region, supporting the notion of using blood tissue DNA methylation as a proxy for DNA methylation changes in the brain [60].

DNA methylation is tissue specific and for brain-related phenotypes such as CPSP, careful consideration of tissue source for epigenetic analyses is important. Use of blood for DNA methylation studies in neural phenotypes is

supported by blood–brain DNA methylation concordance studies which have observed high correlation of DNA methylation levels across tissues especially related to genetic influences [61,62]. Also, a significant overlap of *cis* meQTLs (45–73%) and targeted CpG sites (31–68%) has been reported across brain prefrontal cortex, whole blood and saliva [29]. In fact, cross-tissue meQTLs are also enriched in cross-tissue eQTLs in association with schizophrenia [29]. meQTL maps and cross-tissue meQTLs have previously been examined using data of meQTL and corresponding CpG sites derived from infant cord, blood tissue from children, and publicly available brain tissue databases. The authors found that in subjects with autism spectrum disorder, both peripheral blood and fetal brain were enriched for meQTLs [63]. Similar findings for overlap of, meQTL signals across adult brain and blood tissues [20], further suggest blood-derived meQTLs may serve as biomarkers and represent brain tissue SNP–DNA methylation relationships. This gives us confidence in our blood-based findings in relation to a neural phenotype [64]. Our findings provide a basis for future investigation of brain and blood meQTLs for specifically pain phenotypes.

We will focus our discussion on the PARK16 locus where most of our major findings are. There is prior evidence for the function of variants we identified in PARK16 locus (rs960603 and rs708723) as meQTLs. Our results show that rs960603 A allele on *PM20D1* is associated with increased risk for CPSP and increased DNA methylation at CpG sites on PM20*D*1. The direction of meQTL-DNA methylation associations are aligned with previous studies which found an association between *PM20D1* hypermethylation and Alzheimer's disease. They showed that *PM20D1* methylation in human frontal brain cortex samples are dependent on the rs708727– rs960603 haplotype [53]. They observed an allele-dependent correlation with *PM20D1* promoter methylation (TT associated with increased DNA methylation) and further, that *PM20D1* expression was inversely correlated with the methylation of its promoter. In fact, DNA methylation at the same CpG site (cg14893161; Chr 1: 205,819,251) is also affected by rs708723 and rs960603 in our study. Sanchez-Mut *et al.* also used ChIP assays and 3-C assays to show that meQTLs regulate long-range chromatin interaction of the *RAB29-PM20D1* loci and reduce CTCF binding to 3C anchors in human frontal cortex samples with highly methylated at the *PM20D1* promoter (cg14893161). In addition, they demonstrated that transcriptionally silent chromatin state could be restored upon use of DNA demethylating agent 5-aza-2'-deoxycytidine, in turn affecting the chromatin loop and *PM20D1* expression. Thus, in Alzheimer's disease, when *PM20D1* CpG sites are non-methylated, an enhancer region 60 kb downstream of *PM20D1* physically interacts with *PM20D1* promoter via CTCF binding and favors *PM20D1* transcription, which is protective; and hypermethylation is associated with pathology. Similarly, in CPSP, we hypothesize *PM20D1* meQTL effects through hypermethylation at CpG sites increase risk for CPSP, although the mechanism is yet unknown.

A two stage meta-analysis found rs708723/1q32 T allele in *RAB29* increased PD risk [57]. They tested whether association of rs708723 with gene expression and DNA methylation status of proximal transcripts or CpG sites respectively. They found correlations of T > C with increased expression of *NUCKS1* (p = 1.8 × 10 - 7) and decreased expression of *RAB7L1* (p = 7.2 × 10 - 4) in frontal cortex and cerebellar tissue, thus revealing potential biological consequences of this variant. Our study provides further evidence that association of phenotype risk (in our case, CPSP) with rs708723 A (or T) allele in *RAB29* (Chr 1: 205739266) is mediated by decreased DNA methylation at CpG sites at *RAB7L1* and increased DNA methylation at CpG sites at *PM20D1* thus providing a molecular mechanism for the associations between SNP-gene expression. Another study investigating DNA methylation and gene expression in in frontal cortex and cerebellar regions in subjects with PD supports our findings that higher odds for CPSP for meQTL rs823114 G > A on *NUCKS1* was mediated through increased DNA methylation at CpG sites in *PM20D1*. This study reported that the PD risk allele (T) at rs823118 (in LD with rs823114) was associated with increased methylation at *PM20D1*. In addition, they showed PD associated decreased expression of *NUCKS1* and increased transcription of *RAB7L1* in brain tissues [65]. Thus, there seems to be consistency in mechanisms and roles of meQTLs/DNA methylation at PARK16 locus for CPSP and other neurologic conditions.

In addition, there is prior evidence for the role of the genes in the PARK16 locus in pain pathology. *RAB7L1* is a small cytosolic GTPase belonging to the RAB-related GTP-binding protein subfamily [66] has been implicated in intracellular cell signaling processes and vesicle trafficking [67]. While in gene knockdown mice, significantly decreased neurite process length was found [56] overexpression was protective against alpha-syn-induced dopaminergic neuronal loss in animal models of PD [68]. This would suggest increased expression was protective for CPSP. However, gain-of-function mutations in *RAB7* were proposed to cause Charcot–Marie–Tooth type 2B neuropathy, a disorder characterized by sensory loss [69] with increased lysosomal activity, autophagy and premature degradation of long axons due to trafficking of neurotrophic factors and prolonged mitogen-activated protein kinase activation

in the long axons of peripheral sensory neurons [70]. Given the conflicting mechanisms for *RAB7L1* in PD and Charcot–Marie–Tooth, there is much to be known about its mechanistic role in CPSP. Interestingly, *PM20D1* codes for PM20D1, a factor secreted by thermogenic adipose cells that catalyzes both the hydrolysis and condensation of N-acyl amino acids, which have been found to play a role in nociception [71]. *PM20D1*-knockout mice were shown to have bidirectional changes in N-acyl amino acid levels in blood/tissues and influence late nociceptive behaviors in mice in formalin assay models [72]. This is aligned with our observations that increased DNA methylation of *PM20D1* (decreased expression) increased CPSP risk. The differences in early and late nociceptive effects of *PM20D1* may support the use of *PM20D1* inhibitors for acute but not chronic pain management [72].

The key link between DNA methylation and gene expression is related to chromatic accessibility and TFBS. TFs play an important role in altering gene expression in response to injury, stress and other events influencing neuronal plasticity and pain [73]. Using bioinformatics enrichment methods to integrate chromatin state and TF binding profiles with DNA methylation profiles, we identified functional meQTLs [74]. We conducted ATAC-seq experiments which showed the presence of chromatin accessibility peaks in CpG rich areas as well as verified CTCF binding sites in PARK16 locus by use of overlapping ChIP-seq data from ENCODE. There is recent evidence that >95% CTCF sites bound by cohesin mediate chromatin looping [75] and regulates chromatin accessibility and transcription [76]. The CTCF site has in fact been previously identified as a key area involved in long-range interactions with meQTLs rs708723 (*RAB7L1*) and rs960603 (*PM20D1*) [53]. Our study identified rs960603 and rs708727 as meQTLs to also be associated with CPSP. In addition, Homer bioinformatics analyses showed enrichment for repressive histone marks and TF binding sites at CpG sites with significant enrichment for MAF, Zinc finger proteins, GATA and homeodomain family TF. In a case-control study of 5 PARK16 locus (*RAB7L1* and *SLC41A1*) variants for PD, which found them to be protective, a putative GATA1 binding site was previously identified that is potentially altered by variants in the promoter region of *RAB7L1* [77], consistent with our results showing enrichment for GATA1 binding sites at the 127 CpGs that causally mediate associations between SNPs and CPSP (Figure 3B). In another study, the allele rs823144 A >C within the PARK16 locus was found to be protective for PD, with differential binding of particular TFs proposed to contribute to altered expression levels of the *RAB7L1* gene [55]. Our findings of DNA methylation mediating association of meQTLs with phenotype (CPSP) provides a plausible putative mechanism for altered TFBS at this locus for neural phenotypes involving dopaminergic processes.

We used CIT to further examine which of the CpG sites may be causal mediators of SNP-CPSP associations. A limitation of this study is the relatively low standards when selecting putative candidate sites. Due to the exploratory nature of the study and small sample size, no priori power analysis or correction on multiple testing was conducted. In compensation, we took the methylation difference into account. Only sites that showed at least 5% difference between groups were considered. Our previous study demonstrated that this strategy could be effective and sometimes more critical in the identification of differentially methylated positions [39]. Replication studies are needed to draw any solid conclusions. While there are challenges to applying CIT methods related to low power of multiple testing; simulation studies have demonstrated the validity and advantage of the CIT package over other common multiple testing strategies [38]. The functional interpretation of our study results are limited by the absence of experimental data from relevant cell lines and expression data, given that meQTLs are enriched in regulatory domains and are known to both enhance and repress gene expression in a cell- and tissue-specific way. Hence, we verified using G-TEx portal that meQTLs associated with increased DNA methylation was associated with decreased gene expression for *PM20D1* (eQTLs) in brain and blood tissue, and vice versa for *RAB7L1* with no effect on expression of other PARK16 genes. Cellular heterogeneity presents a major confounding factor in epigenetic studies. We used statistical methods (surrogate variable analysis (SVA 3.24.4)) to control batch effect and unknown confounders such as cell composition [16,78,79]. We would like to point out that by using a study cohort with minimal preoperative pain, our study design has the advantage of mitigating time dependent cause–effect questions that usually complicates DNA methylation-phenotype relationships in acute to chronic pain transitions.

Conclusion

meQTLs analysis in blood suggest potential novel molecular mechanisms mediating genetic associations with CPSP. They also partially explain molecular function of non-protein-coding, CPSP associated genetic variants. What is not known is whether meQTL associated CpG sites are also subject to environmental effects and if so, the proportion of gene-environmental effects [80]. If the effects on DNA methylation are purely genetic, this will need to be considered in future epigenetic studies.

Future perspective

While genetic variation (meQTL) cannot currently be modified, DNA methylation may be a modifiable risk factor. Understanding epigenetic-mediating mechanisms opens the possibility of development of targeted therapeutic approaches to reprogram these modifications. The identification of TFBS associated with the meQTLs in previously known pain and dopamine function relevant genetic loci such as PARK16 renders new avenues to regulate their function and could spur new research into biomarkers and modifiable strategies in genetically susceptible individuals. Our study provides novel pilot data for future transcriptome and TF binding studies to evaluate key DNA methylation sites. Future multi-omics studies of gene expression are needed to validate our findings and identify the SNP-DNA methylation-mRNA associations in relation to CPSP and chromatin structure profiles to identify functional meQTLs [81]. Single-cell assays and programmable nucleases could be used to further explore the function of non-coding variants on DNA methylation [82], and environmental stimuli exposure could be tested to understand how meQTLs encode environmental interactions by regulating DNA methylation.

Summary points

- By integrating genotype-DNA methylation and bioinformatics data, our pilot study identified putative methylation quantitative trait locis (meQTLs) and investigated DNA methylation as a mediator of genetic variant associations with chronic postsurgical pain.
- 2753 meQTL associated with DNA methylation at 480 cytosine–guanine dinucleotide (CpG) sites were identified ($p < 0.05$; $\geq 5\%$ change in DNA methylation).
- DNA methylation at 127 CpGs mediated associations between 470 single nucleotide polymorphisms and chronic postsurgical pain (CPSP).
- Functional genomics analyses identified enrichment for repressive histone marks and transcription factors (MAF, KLF1, FOXC1) binding sites at the CpG sites, providing putative evidence for altered binding events due to differential methylation, which need further experimental validation.
- meQTLs in blood may partially explain molecular function of non-protein-coding, CPSP associated genetic variants.
- PARK16 gene locus (spans five genes, has known dopamine regulating effects) was enriched for meQTL-CpG pairs after CIT. Hypomethylation at CG sites at *RAB7L1* and hypermethylation of CG sites at *PM20D1* within PARK16 locus mediated association of meQTLs (for example, *RAB7L1* (rs708723), *PM20D1* (rs960603) and *NUCKS1* (rs823114)) with CPSP. Corresponding meQTLs were identified for *RAB7L1* and *PM20D1* using G-TEx.
- ATAC-seq identified accessible chromatin at differentially methylated CpG locations at PARK16 and CTCF-binding site which has been previously identified as a key area involved in long-range interactions with meQTLs rs708727 (*RAB7L1*) and rs960603 (*PM20D1*.
- Replication to bolster the pilot findings of this study and future studies detailing meQTL-DNA methylation-gene expression-CPSP relation and impacted transcription factor binding sites are needed.

---

or financial involvement with any organization or entity with a financial interest in or financial conflict with the subject matter or materials discussed in the manuscript apart from those disclosed.

No writing assistance was utilized in the production of this manuscript.

Ethical conduct of research

The authors state that they have obtained appropriate institutional review board approval or have followed the principles outlined in the Declaration of Helsinki for all human or animal experimental investigations. In addition, for investigations involving human subjects, informed consent has been obtained from the participants involved.

Data sharing statement

Pilot epigenome-wide and candidate DNAm study results from this cohort have been previously published. The studies are registered with ClinicalTrials.gov (Identifier: NCT01839461, NCT01731873), Individual deidentified participant data (including data dictionaries) has/will be shared; PLINK genotype and phenotype data have been uploaded to dbGAP (accession number phs002105.v1.p1). DNAm data will be uploaded soon.

References

1. Macrae WA, Davies HTO. In: *Epidemiology of pain.* Crombie IK (Ed.). IASP Press, Seattle, 125–142 (1999).

2. Rabbitts JA, Fisher E, Rosenbloom BN, Palermo TM. Prevalence and predictors of chronic postsurgical pain in children: a systematic review and meta-analysis. *J. Pain* 18(6), 605–614 (2017).

3. Thapa P, Euasobhon P. Chronic postsurgical pain: current evidence for prevention and management. *Korean J. Pain* 31(3), 155–173 (2018).

4. Katz J, Seltzer Z. Transition from acute to chronic postsurgical pain: risk factors and protective factors. *Expert Rev. Neurother.* 9(5), 723–744 (2009).

5. Clarke H, Katz J, Flor H, Rietschel M, Diehl SR, Seltzer Z. Genetics of chronic post-surgical pain: a crucial step toward personal pain medicine. *Can. J. Anaesth.* 62(3), 294–303 (2015).

6. Chidambaran V, Gang Y, Pilipenko V, Ashton M, Ding L. Systematic review and meta-analysis of genetic risk of developing chronic postsurgical pain. *J. Pain* 21(1-2), 2–24 (2020)

7. Warner SC, Van Meurs JB, Schiphof D *et al.* Genome-wide association scan of neuropathic pain symptoms post total joint replacement highlights a variant in the protein-kinase C gene. *Eur. J. Hum. Genet.* 25(4), 446–451 (2017).

8. Costigan M, Belfer I, Griffin RS *et al.* Multiple chronic pain states are associated with a common amino acid-changing allele in KCNS1. *Brain* 133(9), 2519–2527 (2010).

9. Hickey OT, Nugent NF, Burke SM, Hafeez P, Mudrakouski AL, Shorten GD. Persistent pain after mastectomy with reconstruction. *J. Clin. Anesth.* 23(6), 482–488 (2011).

10. Montes A, Roca G, Sabate S *et al.* Genetic and clinical factors associated with chronic postsurgical pain after hernia repair, hysterectomy, and thoracotomy: a two-year multicenter cohort study. *Anesthesiology* 122(5), 1123–1141 (2015).

11. Belfer I, Dai F, Kehlet H *et al.* Association of functional variations in COMT and GCH1 genes with postherniotomy pain and related impairment. *Pain* 156(2), 273–279 (2015).

12. Kolesnikov Y, Gabovits B, Levin A *et al.* Chronic pain after lower abdominal surgery: do catechol-O-methyl transferase/opioid receptor mu-1 polymorphisms contribute?. *Mol. Pain* 9, 19 (2013).

13. Bai G, Ren K, Dubner R. Epigenetic regulation of persistent pain. *Transl. Res.* 165(1), 177–199 (2015).

14. Doehring A, Geisslinger G, Lotsch J. Epigenetics in pain and analgesia: an imminent research field. *Eur. J. Pain* 15(1), 11–16 (2011).

15. Denk F, Mcmahon SB. Chronic pain: emerging evidence for the involvement of epigenetics. *Neuron* 73(3), 435–444 (2012).

16. Chidambaran V, Zhang X, Geisler K *et al.* Enrichment of genomic pathways based on differential dna methylation associated with chronic postsurgical pain and anxiety in children: a prospective, pilot study. *J. Pain* 20(7), 771–785 (2019).

17. Chidambaran V, Zhang X, Martin LJ *et al.* DNA methylation at the mu-1 opioid receptor gene (OPRM1) promoter predicts preoperative, acute, and chronic postsurgical pain after spine fusion. *Pharmgenomics Pers. Med.* 10, 157–168 (2017).

18. Chidambaran V, Ashton M, Martin LJ, Jegga AG. Systems biology-based approaches to summarize and identify novel genes and pathways associated with acute and chronic postsurgical pain. *J. Clin. Anesth.* 62, 109738 (2020).

19. Crow M, Denk F, Mcmahon SB. Genes and epigenetic processes as prospective pain targets. *Genome Med.* 5(2), 12 (2013).

20. Smith AK, Kilaru V, Kocak M *et al.* Methylation quantitative trait loci (meQTLs) are consistently detected across ancestry, developmental stage, and tissue type. *BMC Genomics* 15, 145 (2014).

21. Do C, Shearer A, Suzuki M *et al.* Genetic-epigenetic interactions in *cis*: a major focus in the post-GWAS era. *Genome Biol.* 18(1), 120 (2017).

22. Hannon E, Gorrie-Stone TJ, Smart MC *et al.* Leveraging DNA-methylation quantitative-trait loci to characterize the relationship between methylomic variation, gene expression, and complex traits. *Am. J. Hum. Genet.* 103(5), 654–665 (2018).

23. Banovich NE, Lan X, Mcvicker G *et al.* Methylation QTLs are associated with coordinated changes in transcription factor binding, histone modifications, and gene expression levels. *PLoS Genet.* 10(9), e1004663 (2014).

24. Maurano MT, Humbert R, Rynes E *et al.* Systematic localization of common disease-associated variation in regulatory DNA. *Science* 337(6099), 1190–1195 (2012).

25. Hannon E, Spiers H, Viana J *et al.* Methylation QTLs in the developing brain and their enrichment in schizophrenia risk loci. *Nat. Neurosci.* 19(1), 48–54 (2016).

26. Tang Y, Jin B, Zhou L, Lu W. MeQTL analysis of childhood obesity links epigenetics with a risk SNP rs17782313 near MC4R from meta-analysis. *Oncotarget* 8(2), 2800–2806 (2017).

27. Rushton MD, Reynard LN, Young DA *et al.* Methylation quantitative trait locus analysis of osteoarthritis links epigenetics with genetic risk. *Hum. Mol. Genet.* 24(25), 7432–7444 (2015).

28. Zhang H, Wang F, Kranzler HR *et al.* Identification of methylation quantitative trait loci (mQTLs) influencing promoter DNA methylation of alcohol dependence risk genes. *Hum. Genet.* 133(9), 1093–1104 (2014).

29. Lin D, Chen J, Perrone-Bizzozero N *et al.* Characterization of cross-tissue genetic-epigenetic effects and their patterns in schizophrenia. *Genome Med.* 10(1), 13 (2018).

30. Von Baeyer CL. Numerical rating scale for self-report of pain intensity in children and adolescents: recent progress and further questions. *Eur. J. Pain* 13(10), 1005–1007 (2009).

31. Silverman WK, Fleisig W, Rabian B, Peterson RA. Childhood anxiety sensitivity index. *J. Clin. Child Psychol.* 20, 162–168 (1991).

32. Chidambaran V, Ding L, Moore DL *et al.* Predicting the pain continuum after adolescent idiopathic scoliosis surgery: a prospective cohort study. *Eur. J. Pain* 21(7), 1252–1265 (2017).

33. Gerbershagen HJ, Rothaug J, Kalkman CJ, Meissner W. Determination of moderate-to-severe postoperative pain on the numeric rating scale: a cut-off point analysis applying four different methods. *Br. J. Anaesth.* 107(4), 619–626 (2011).

34. Wang K, Li M, Hakonarson H. ANNOVAR: functional annotation of genetic variants from high-throughput sequencing data. *Nucleic Acids Res.* 38(16), e164–e164 (2010).

35. Purcell S, Neale B, Todd-Brown K *et al.* PLINK: a tool set for whole-genome association and population-based linkage analyses. *Am. J. Hum. Genet.* 81(3), 559–575 (2007).

36. Shabalin AA. Matrix eQTL: ultra fast eQTL analysis via large matrix operations. *Bioinformatics* 28(10), 1353–1358 (2012).

37. Millstein J, Zhang B, Zhu J, Schadt EE. Disentangling molecular relationships with a causal inference test. *BMC Genet.* 10(1), 23 (2009).

38. Millstein J, Chen GK, Breton CV. cit: hypothesis testing software for mediation analysis in genomic applications. *Bioinformatics* 32(15), 2364–2365 (2016).

39. Zhang X, Chen X, Weirauch MT *et al.* Diesel exhaust and house dust mite allergen lead to common changes in the airway methylome and hydroxymethylome. *Environ Epigenet* 4(3), dvy020 (2018).

40. Consortium EP. An integrated encyclopedia of DNA elements in the human genome. *Nature* 489(7414), 57–74 (2012).

41. Chadwick LH. The NIH Roadmap Epigenomics Program data resource. *Epigenomics* 4(3), 317–324 (2012).

42. Grubert F, Zaugg JB, Kasowski M *et al.* Genetic control of chromatin states in humans involves local and distal chromosomal interactions. *Cell* 162(5), 1051–1065 (2015).

43. Harley JB, Chen X, Pujato M *et al.* Transcription factors operate across disease loci, with EBNA2 implicated in autoimmunity. *Nat. Genet.* 50(5), 699–707 (2018).

44. Heinz S, Benner C, Spann N *et al.* Simple combinations of lineage-determining transcription factors prime *cis*-regulatory elements required for macrophage and B cell identities. *Mol. Cell* 38(4), 576–589 (2010).

45. Weirauch MT, Yang A, Albu M *et al.* Determination and inference of eukaryotic transcription factor sequence specificity. *Cell* 158(6), 1431–1443 (2014).

46. Fragiadakis GK, Gaudillière B, Ganio EA *et al.* Patient-specific immune states before surgery are strong correlates of surgical recovery. *Anesthesiology* 123(6), 1241–1255 (2015).

47. Gaudilliere B, Fragiadakis GK, Bruggner RV *et al.* Coordinated surgical immune signatures contain correlates of clinical recovery. *Sci. Transl. Med.* 6(255), 255ra131–255ra131 (2014).

48. Corces MR, Trevino AE, Hamilton EG *et al.* An improved ATAC-seq protocol reduces background and enables interrogation of frozen tissues. *Nat. Methods* 14(10), 959–962 (2017).

49. Kartashov AV, Barski A. BioWardrobe: an integrated platform for analysis of epigenomics and transcriptomics data. *Genome Biol.* 16, 158 (2015).

50. Langmead B, Trapnell C, Pop M, Salzberg SL. Ultrafast and memory-efficient alignment of short DNA sequences to the human genome. *Genome Biol.* 10(3), R25 (2009).

51. Zhang Y, Liu T, Meyer CA *et al.* Model-based analysis of ChIP-Seq (MACS). *Genome Biol.* 9(9), R137 (2008).

52. Ji H, Ehrlich LI, Seita J *et al.* Comprehensive methylome map of lineage commitment from haematopoietic progenitors. *Nature* 467(7313), 338–342 (2010).

53. Sanchez-Mut JV, Heyn H, Silva BA *et al.* PM20D1 is a quantitative trait locus associated with Alzheimer's disease. *Nat. Med.* 24(5), 598–603 (2018).

54. Pihlstrom L, Rengmark A, Bjornara KA *et al.* Fine mapping and resequencing of the PARK16 locus in Parkinson's disease. *J. Hum. Genet.* 60(7), 357–362 (2015).

55. Khaligh A, Goudarzian M, Moslem A *et al.* RAB7L1 promoter polymorphism and risk of Parkinson's disease; a case-control study. *Neurol. Res.* 39(5), 468–471 (2017).

56. Macleod DA, Rhinn H, Kuwahara T *et al.* RAB7L1 interacts with LRRK2 to modify intraneuronal protein sorting and Parkinson's disease risk. *Neuron* 77(3), 425–439 (2013).

57. Satake W, Nakabayashi Y, Mizuta I *et al.* Genome-wide association study identifies common variants at four loci as genetic risk factors for Parkinson's disease. *Nat. Genet.* 41(12), 1303–1307 (2009).

58. Blanchet PJ, Brefel-Courbon C. Chronic pain and pain processing in Parkinson's disease. *Prog. Neuropsychopharmacol. Biol. Psychiatry* 87(Pt B), 200–206 (2018).

59. Serafini RA, Pryce KD, Zachariou V. The mesolimbic dopamine system in chronic pain and associated affective comorbidities. *Biol. Psychiatry* 87(1), 64–73 (2020).

60. Prasad R, Jho EH. A concise review of human brain methylome during aging and neurodegenerative diseases. *BMB Rep.* 52(10), 577–588 (2019).

61. Davies MN, Volta M, Pidsley R *et al.* Functional annotation of the human brain methylome identifies tissue-specific epigenetic variation across brain and blood. *Genome Biol.* 13(6), R43 (2012).

62. Hannon E, Lunnon K, Schalkwyk L, Mill J. Interindividual methylomic variation across blood, cortex, and cerebellum: implications for epigenetic studies of neurological and neuropsychiatric phenotypes. *Epigenetics* 11, 10 (2015).

63. Andrews SV, Ellis SE, Bakulski KM *et al.* Cross-tissue integration of genetic and epigenetic data offers insight into autism spectrum disorder. *Nat. Commun.* 8(1), 1011 (2017).

64. Huan T, Joehanes R, Song C *et al.* Genome-wide identification of DNA methylation QTLs in whole blood highlights pathways for cardiovascular disease. *Nat. Commun.* 10(1), 4267 (2019).

65. Nalls MA, Pankratz N, Lill CM *et al.* Large-scale meta-analysis of genome-wide association data identifies six new risk loci for Parkinson's disease. *Nat. Genet.* 46(9), 989–993 (2014).

66. Shimizu F, Katagiri T, Suzuki M *et al.* Cloning and chromosome assignment to 1q32 of a human cDNA (RAB7L1) encoding a small GTP-binding protein, a member of the RAS superfamily. *Cytogenet. Cell Genet.* 77(3–4), 261–263 (1997).

67. Grill B, Bienvenut WV, Brown HM, Ackley BD, Quadroni M, Jin Y. C. elegans RPM-1 regulates axon termination and synaptogenesis through the Rab GEF GLO-4 and the Rab GTPase GLO-1. *Neuron* 55(4), 587–601 (2007).

68. Cooper AA, Gitler AD, Cashikar A *et al.* α-Synuclein blocks ER-golgi traffic and Rab1 rescues neuron loss in Parkinson's models. *Science* 313(5785), 324–328 (2006).

69. Verhoeven K, De Jonghe P, Coen K *et al.* Mutations in the small GTP-ase late endosomal protein RAB7 cause Charcot-Marie-Tooth type 2B neuropathy. *Am. J. Hum. Genet.* 72(3), 722–727 (2003).

70. Liu H, Wu C. Charcot Marie Tooth 2B peripheral sensory neuropathy: How Rab7 mutations impact NGF signaling? *Int. J. Mol. Sci.* 18(2), 324 (2017).

71. Huang SM, Bisogno T, Petros TJ *et al.* Identification of a new class of molecules, the arachidonyl amino acids, and characterization of one member that inhibits pain. *J. Biol. Chem.* 276(46), 42639–42644 (2001).

72. Long JZ, Roche AM, Berdan CA *et al.* Ablation of PM20D1 reveals *N*-acyl amino acid control of metabolism and nociception. *Proc. Natl Acad. Sci. USA* 115(29), E6937–E6945 (2018).

73. Woolf CJ, Costigan M. Transcriptional and posttranslational plasticity and the generation of inflammatory pain. *Proc. Natl Acad. Sci. USA* 96(14), 7723–7730 (1999).

74. Rushton MD, Reynard LN, Young DA *et al.* Methylation quantitative trait locus analysis of osteoarthritis links epigenetics with genetic risk. *Hum. Mol. Genet.* 24(25), 7432–7444 (2015).

75. Pugacheva EM, Kubo N, Loukinov D *et al.* CTCF mediates chromatin looping via N-terminal domain-dependent cohesin retention. *Proc. Natl Acad. Sci. USA* 117(4), 2020–2031 (2020).

76. Holwerda S, De Laat W. Chromatin loops, gene positioning, and gene expression. *Front. Genet.* 3, 217 (2012).

77. Gan-Or Z, Bar-Shira A, Dahary D *et al.* Association of sequence alterations in the putative promoter of RAB7L1 with a reduced Parkinson disease risk. *Arch. Neurol.* 69(1), 105–110 (2012).

78. Leek JT, Johnson WE, Parker HS, Jaffe AE, Storey JD. The sva package for removing batch effects and other unwanted variation in high-throughput experiments. *Bioinformatics* 28(6), 882–883 (2012).

79. Leek JT, Johnson WE, Parker HS, *et al.* Sva: surrogate variable analysis. *Bioinformatics* 28(6), 882–883 (2012).

80. Lim IY, Lin X, Karnani N. Implications of genotype and environment on variation in dna methylation. In: *Handbook of Nutrition, Diet, and Epigenetics* Patel V, Preedy V (Eds). Springer International Publishing, Cham, Switzerland, 1–20 (2017).

81. Lu Y-H, Wang B-H, Jiang F *et al.* Multi-omics integrative analysis identified SNP-methylation-mRNA: interaction in peripheral blood mononuclear cells. *J. Cell. Mol. Med.* 23(7), 4601–4610 (2019).

82. Farlik M, Sheffield NC, Nuzzo A *et al.* Single-cell DNA methylome sequencing and bioinformatic inference of epigenomic cell-state dynamics. *Cell Rep.* 10(8), 1386–1397 (2015).